Science of the Total Environment 807 (2022) 150536

Contents lists available at ScienceDirect

Science of the Total Environment

journal homepage: www.elsevier.com/locate/scitotenv

COVID-19 in New York state: Effects of demographics and air quality on infection and fatality

Sumona Mondal [a,1], Chaya Chaipitakporn [b,1], Vijay Kumar [a], Bridget Wangler [b], Supraja Gurajala [c], Suresh Dhaniyala [d], Shantanu Sur [e,*]

[a] Department of Mathematics, Clarkson University, Potsdam, NY, USA
[b] David D. Reh School of Business, Clarkson University, Potsdam, NY, USA
[c] Department of Computer Science, SUNY Potsdam, Potsdam, NY, USA
[d] Department of Mechanical and Aeronautical Engineering, Clarkson University, Potsdam, NY, USA
[e] Department of Biology, Clarkson University, Potsdam, NY, USA

HIGHLIGHTS

- The impact of COVID-19 varied widely across the counties in the state of New York during the first pandemic wave.
- Long-term exposure to higher $PM_{2.5}$ is associated an increased infection, mortality, and fatality.
- Distance from the disease epicenter strongly influences COVID-19 infection burden.
- Increased age (>55 year) is found to be the strongest predictor for COVID-19 fatality.

GRAPHICAL ABSTRACT

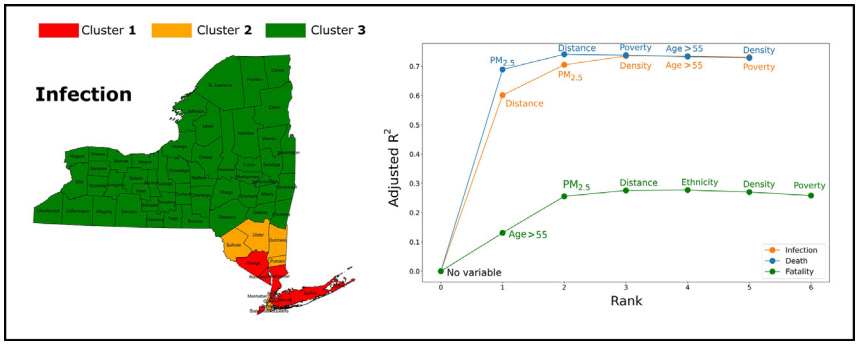

ARTICLE INFO

Article history:
Received 10 March 2021
Received in revised form 28 July 2021
Accepted 19 September 2021
Available online 24 September 2021

Editor: Sheridan Scott

Keywords:
COVID-19
New York state
Air quality
$PM_{2.5}$
Clustering
Stepwise regression

ABSTRACT

The coronavirus disease 2019 (COVID-19) has had a global impact that has been unevenly distributed among and even within countries. Multiple demographic and environmental factors have been associated with the risk of COVID-19 spread and fatality, including age, gender, ethnicity, poverty, and air quality among others. However, specific contributions of these factors are yet to be understood. Here, we attempted to explain the variability in infection, death, and fatality rates by understanding the contributions of a few selected factors. We compared the incidence of COVID-19 in New York State (NYS) counties during the first wave of infection and analyzed how different demographic and environmental variables associate with the variation observed across the counties. We observed that infection and death rates, two important COVID-19 metrics, to be highly correlated with both being highest in counties located near New York City, considered as one of the epicenters of the infection in the US. In contrast, disease fatality was found to be highest in a different set of counties despite registering a low infection rate. To investigate this apparent discrepancy, we divided the counties into three clusters based on COVID-19 infection, death, or fatality, and compared the differences in the demographic and environmental variables such as ethnicity, age, population density, poverty, temperature, and air quality in each of these clusters. Furthermore, a regression model built on this data reveals $PM_{2.5}$ and distance from the epicenter are significant risk factors for infection, while disease fatality has a strong association with age and $PM_{2.5}$. Our results

* Corresponding author.
E-mail address: ssur@clarkson.edu (S. Sur).
[1] These authors contributed equally to this work.

https://doi.org/10.1016/j.scitotenv.2021.150536

demonstrate that for the NYS, demographic components distinctly associate with specific aspects of COVID-19 burden and also highlight the detrimental impact of poor air quality. These results could help design and direct location-specific control and mitigation strategies.

1. Introduction

The impact of the COVID-19 pandemic on global health and economy has exceeded well over the severity of any other communicable diseases in recent history (Baldwin and Di Mauro, 2020; Sarkodie and Owusu, 2020a). The pandemic has also stimulated and significantly accelerated global research into coronaviruses, airborne disease transmissions, and development of new vaccines. Within a short span of time, scientists have succeeded in obtaining critical information on the structure and genomic sequence of the virus pathogen SARS-CoV-2, mechanism of virus infection to host, modes of transmission, and injury to host organs induced by the virus. The research findings have accelerated the development of vaccines and established preventive measures such as the use of masks. Simultaneously, there has been a significant effort to understand the association of COVID-19 to demographic and environmental factors to explain the geographical or seasonal variability in disease burden (Goldstein and Lee, 2020; Karmakar et al., 2021; Perone, 2021; Sorci et al., 2020). Underscoring precise influences of human demographics and environmental factors on the pandemic would be important toward developing effective public health and social measures.

Among the demographic variables, age, gender, ethnicity, and population density are reported to impact COVID-19. Advanced age is shown to significantly increase the fatality from COVID-19. A study conducted on hospitalized patients in the New York City (NYC) area found 84% of the total deaths occurred in people aged above 60 years (Mesas et al., 2020; Richardson et al., 2020). Moreover, males were seen to be more susceptible to suffer from COVID-19 complications and fatality (Pradhan and Olsson, 2020). Although the mechanism underlying such predisposition of age and sex is not completely understood, the presence of preexisting health conditions and a lowered immunity associated with higher age are thought to be two major factors (Mesas et al., 2020; Pradhan and Olsson, 2020; Richardson et al., 2020). Chronic comorbidities such as hypertension, ischemic heart disease, diabetes, and chronic obstructive pulmonary disease (COPD) are more common in older age and poses risk for severe outcomes (Lusignan et al., 2020; Richardson et al., 2020). Studies focused on the impact of COVID-19 on the ethnic composition also revealed vulnerabilities of certain ethnicities to the disease. In the US, a disproportionately higher number of COVID-19 infections and deaths are observed among African Americans and Hispanic Americans relative to their share of population (Martinez et al., 2020; Yancy, 2020). Socioeconomic disparities leading to increased exposure and lower access to healthcare are thought to contribute to such vulnerability. High population density is reported to increase the risk of COVID-19 spread (Arif and Sengupta, 2020; Copiello and Grillenzoni, 2020), although it is not the sole determining factor as many dense metropolitan cities in Japan, South Korea, China, and Singapore have observed a low infection rate (Lee et al., 2020; Rocklöv and Sjödin, 2020).

The association of environmental factors such as air quality and meteorological parameters to the adverse effects of COVID-19 has been investigated in multiple studies. Air pollution is of particular interest as chronic exposure to air pollutants is linked to multiple chronic respiratory and cardiovascular diseases such as COPD, ischemic heart disease, and hypertension—diseases which are known to increase COVID-19 fatality (Feng et al., 2016b; Guan et al., 2016; Wellenius et al., 2012). Additionally, air pollution substantially increases the risk of respiratory infections including viral infections (Chauhan and Johnston, 2003; Feng et al., 2016a). Fine particulate matter in the air, especially $PM_{2.5}$ (particulate matter with aerodynamic diameter 2.5 μm or less) has been linked to many of these pollution-mediated health effects (Brook et al., 2010; Hopke et al., 2019; Xing et al., 2016). Early reports indicate a positive association of $PM_{2.5}$ with both COVID-19 transmission and fatality (Gupta et al., 2020; Lolli et al., 2020; Pozzer et al., 2020; Wu et al., 2020). Analysis of meteorological factors based on the data from 30 Chinese cities revealed low temperature, less diurnal temperature variation, and low humidity favor the transmission of COVID-19 infection (Liu et al., 2020). This finding was supported by a larger-scale study using data from the top 20 countries with infections, and further claimed low wind speed, surface pressure, and precipitation to increase the risk of disease spread (Sarkodie and Owusu, 2020b).

While the connection of COVID-19 with demographic and environmental factors has been demonstrated by multiple studies, majority of these studies focused on disease transmission or disease fatality alone, and the analyses were directed to either the demographic or the environmental variables. Since anthropogenic factors have a substantial impact on the environmental variables, consideration of both demographic and environmental factors in the analysis is expected to increase the robustness of inference and reduce the risk of any spurious association (Copiello and Grillenzoni, 2020). Collating information from existing studies to understand the relative impact of these risk factors on infection burden and disease fatality is challenging since these studies were conducted in different geographical locations, and multiple additional confounding factors such as testing and screening strategies, healthcare infrastructure, and socio-cultural practices could contribute to the wide variability of COVID-19 infection and fatality observed across countries or even between different regions within a country (Auger et al., 2020; Chen and Krieger, 2021; Miller et al., 2020). Therefore, to assess the influence of both demographic and environmental factors on COVID-19, ideally the data should be from a geographical location where these factors show considerable variation with low variability of other confounding factors. New York State (NYS), located in the USA, fits well as a potential location to conduct such study, as it offers a wide range of variation in its demographic landscapes from urban, population-dense, ethnically diverse counties near NYC to many rural, white-dominated, population-sparse counties located in the upstate region. The $PM_{2.5}$ distribution across the state demonstrates a consistent pattern with distinct variation across regions (Jin et al., 2019). Additionally, state-wide implemented policies, including public health measures and hospital care would help to reduce the potential differences due to the confounding factors mentioned above. Analyses conducted in the NYC area revealed that multiple demographic factors such as ethnicity, male gender, poverty, and household crowding are associated with increased COVID-19 infection, hospitalization, or death (Chen and Krieger, 2021; Reichberg et al., 2020). Studies from NYC metropolitan area also suggested a potential connection of air quality and meteorological variables such as temperature and humidity to higher COVID-19 transmission (Adhikari and Yin, 2020; Bashir et al., 2020). Inclusion of data from the entire NYS is expected to capture a wider variability of these variables and provide a deeper insight into their role in the COVID-19 burden.

In this work, we considered the NYS data at county-level resolution and attempted to relate the variability in infection, death, and fatality with selected demographic and environmental factors during the first COVID-19 wave. Using publicly available data, we first grouped the counties into clusters based on COVID-19 infection, death, or fatality rates during the study period, and investigated the association of these clusters with various demographic factors (e.g., population density, the proportion of African American and Hispanic American

population) and environmental factors (e.g., $PM_{2.5}$ and temperature). To identify the risk variables that have major contributions on specific aspects of COVID-19 burden, regression models were then built using data from individual counties, where infection, death, or fatality rates were considered as response variables while demographic and environmental factors were used as predictor variables.

2. Methods

2.1. Study area, data source, and variables

For this study, COVID-19 infection and death count during the period of March 1, 2020, to May 16, 2020, were obtained for all 62 counties in the NYS from publicly accessible information available at Syracuse.com (Table 1). The population estimates for each county were obtained from the 2018 US Census Bureau's American Community Survey (ACS) website (https://www.census.gov/programs-surveys/acs) (U.S. Census Bureau ACS, 2018). Infection and death rates from COVID-19 for each county were calculated by dividing the cumulative infection and cumulative death counts during the study period by the total population of the county, and expressed as number per 100,000 population. The fatality rate of a county was obtained by dividing the cumulative death count by cumulative infection count during the study period and presented as the number of deaths per 10,000 infected population. In addition to the total population, the ACS census database was used to collect the following information for each county:(1) Area; (2) population with age ≥ 55 years; (3) poverty levels; (4) Hispanic American population (Martinez et al., 2020); and (5) African American population (Yancy, 2020). From this information (1) population density (population/mile^2), (2) proportion of the population with ≥55 years (expressed as %), (3) proportion of Hispanic American (expressed as %), and (4) proportion of African American (expressed as %) population was calculated for each county. All factors except population density and distance from the epicenter were converted to percentages by county. The nursing home locations across the NYS counties were obtained from the Department of Health and Human Services. The data was retrieved through ArcGIS Map 10.7.1 (Monmonier and Giordano, 1998). The distance of a county from Manhattan, located at the center of NYC (considered as the disease epicenter (Reichberg et al., 2020; Wadhera et al., 2020)), was used as the distance of the county from the disease epicenter and was calculated by measuring the distance between the centroids of two locations using ArcGIS Map 10.7.1 software. The temperature and Air Quality Index (AQI) information were obtained from Environmental Protection Agency (EPA) measurements available through the United States EPA website (http://www.epa.gov/ttn/airs/aqsdatamart). Hourly outdoor temperature and daily AQI data collected by EPA over a span of 5 years (2015–2019) were used in this study. For county-level $PM_{2.5}$ estimates, temporally averaged $PM_{2.5}$ data previously published by Wu et al. (2020) were used in this study. Briefly, the monthly averages of $PM_{2.5}$ estimates over the entire US were made at 0.1° X 0.1° grid resolution through a combination of satellite-derived estimates, ground-based measurements, and their statistical fusion through a geographically weighted regression model (Donkelaar et al., 2019). This data was further aggregated to the geographical confinement of a county and temporally averaged for the years 2000–2016 to obtain a single $PM_{2.5}$ estimate for each county (Wu et al., 2020). We used this average $PM_{2.5}$ data from the past years in the current study. While the exact mechanisms by which $PM_{2.5}$ influences COVID-19 are not fully understood yet, our choice of average $PM_{2.5}$ from past years is motivated by the findings of multiple studies that point to the association of historical exposure of $PM_{2.5}$ to the disease (Gupta et al., 2020; Maleki et al., 2021; Wu et al., 2020).

Table 1
Publicly available data sources used in this study.

Data	Source
Covid-19 cases & deaths	Coronavirus in NY: Cases, maps, charts, and resources (https://www.syracuse.com/coronavirus-ny/)
Population estimates & demographics 2018	US Census Bureau's American Community Survey (ACS (https://www.census.gov/programs-surveys/acs)
Temperature & air quality index	EPA (http://www.epa.gov/ttn/airs/aqsdatamart)
Nursing homes locations	The Department of Health and Human Services (HHS) (https://www.arcgis.com/home/item.html?id=b3813b2d3a054c378247bf32bcd8d203)
Satellite $PM_{2.5}$ estimates	Air pollution and COVID-19 mortality in the United States, Harvard University (http://github.com/wxwx1993/PM_COVID)

2.2. Statistical analyses

2.2.1. K-means clustering

The counties in the NYS were classified into three categories using k-means clustering technique. Partitioning the counties into three disjoint clusters on the basis of infection, death, and fatality was performed to explore any common pattern that might exist among the counties classified within a cluster. For the implementation of the clustering algorithm, the value of k was set in advance along with the assignment of initial centroid positions for the clusters (Fahim et al., 2006). The algorithm started with the random initialization of the positions of centroids and was followed by two steps. The first step assigned each sample to its nearest centroid. The second step created a new centroid by taking the mean value of all the samples assigned to each previous centroid. The differences between the old and the new centroids were computed, and the algorithm repeated these last two steps until this difference was less than a threshold. The model used Euclidean distance for the calculation of the distance and the threshold considered was 0.0001. In the end, the centroids were fixed, did not move anymore, signifying the convergence criterion for clustering, and resulted in three distinct clusters. Clustering for infection and death was performed using the infection and death rate values from each county. To cluster the counties for fatality, k-means clustering technique was implemented on infection and fatality rate, considering them as two dimensions. Clusters of counties constructed this way were used to study the association with demographic and environmental risk factors.

2.2.2. Tests for significance

Statistical comparisons of demographic and environmental variables between the clusters were performed using Kruskal-Wallis (KW) test, a non-parametric equivalent of one-way analysis of variance (ANOVA), since the data were non-normally distributed. Once the KW test statistic was found to be significant, multiple comparisons were conducted using Mann-Whitney *U* test after making the Bonferroni corrections. All analyses used 2-sided statistical tests and $P < 0.10$ was considered as significant. The Bonferroni correction was set at the significance cut-off value of 0.03.

2.2.3. Autoregressive integrated moving average (ARIMA) model

Temperature and AQI time series data from EPA were used to build ARIMA models to obtain predicted estimates of these variables. Data from one representative EPA site for each of the three clusters in each category of infection, death, and fatality were included in the analysis. The models were constructed using time series data from the years 2015–2019. Hourly outdoor temperature data and daily AQI data collected from EPA were first converted to weekly data before using in the model.

In ARIMA model, the future values of a variable are predicted by a linear combination of past values and errors (Hyndman and Athanasopoulos, 2018). The model is often expressed as ARIMA (p, d, q), where p, d, and q represent the order of auto-regression, the degree of trend difference, and the order of moving average, respectively. The model is essentially a combination of three parts: (1) The first part is the auto-regressive model, which uses the linear combination of past

values of the variable to forecast the next value and is referred as an AR (p) model, an autoregressive model of order p. (2) The second part is the integrated (I), which is computed by taking the difference between the consecutive observations to make the data stationary. (3) The third part is the moving average (MA) model, referred as MA(q) and equivalent to a regression model that involves past forecast errors as predictors. Augmented Dickey-Fuller (ADF) unit-root test was performed prior to model building to confirm the stationarity of each time series data. Predicted time series values with 95% confidence interval were determined for each condition when implementing the ARIMA model. The model goodness of fit was further evaluated by calculating the Akaike information criterion (AIC). Model predicted values for each cluster within a category were used to compare the temporal pattern of temperature and AQI between the clusters.

2.2.4. Regression models

Regression models were built using the data from individual counties of NYS. Three separate models were built where infection, death, and fatality rate were considered as the response variable, while demographic and environmental factors were used as predictor variables for all three models. Variables were first evaluated for normality of distribution by visual inspection of histograms followed by the Shapiro-Wilks test for normality. The univariate method of outlier detection was used to eliminate outliers in the predictors. Correlations between variables were examined by calculating Pearson's correlation coefficients between the predictor and response variables. Multicollinearity between the predictor variables was further examined by computing variance inflation factor (VIF), which measures the inflation in the variances of parameter estimates due to multicollinearity. An upper cut-off value of VIF was set as 5 to minimize the contribution of multicollinearity in our model (Chatterjee and Simonoff, 2013). A stepwise forward selection procedure was implemented to evaluate the contribution of predictor variables in infection, death, and fatality from COVID-19. The forward selection algorithm for stepwise regression starts with an empty model where predictor variables are added sequentially along with the measurement of model accuracy. This process is repeated until all variables are incorporated into the model. The residuals of the regression models were checked for model adequacy and outliers were removed when needed. The goodness of the model is interpreted by the adjusted R^2 value and the contribution of an individual variable is assessed from the order in which the variable was entered in the model. *P* values of the regression coefficients of the predictor variables were used to assess if their incorporation made a meaningful addition to the model.

All analyses were performed using version 3.6.9 of the Python programming language.

3. Results

3.1. Distribution of COVID-19 in NYS counties

The infections and deaths from COVID-19 in the NYS between March 1 and May 16, 2020, were considered in our analysis. This time window roughly corresponds to the first COVID-19 wave observed in the NYS. To understand the distribution of infections and deaths across the counties within the state, we grouped the counties into three clusters based on each of these variables. Infection and death rates were calculated for all 62 counties in the NYS and then the counties were classified into three clusters using k-means clustering technique. Cluster **1** included counties with a high rate of infection or death, cluster **3** incorporated counties with a low rate, and in cluster **2** the rates were intermediate between the other two clusters (Fig. 1A, B). For infections, we observed that the cluster **1**, where the infection numbers ranged 2500–4000 per 100,000 population, consisted of 8 counties (Rockland, Westchester, Bronx, Nassau, Suffolk, Staten Island, Orange, and Queens), all located in close proximity within the downstate NY (Fig. 1C; counties shaded in red). Cluster **2** was formed by 6 counties located near to cluster **1**, namely Ulster, Dutchess, Putnam, Manhattan, Sullivan, and Brooklyn (Fig. 1C; counties shaded in yellow). The counties of upstate NY fell in the cluster **3** (Fig. 1C; counties shaded in green) where the infection rate was <500 per 100,000 population, well below the other two clusters. The clusters for COVID-19 death showed a similar distribution to infection. Four counties in downstate NY, namely Bronx, Queens, Rockland, and Brooklyn were included in the cluster **1** with death rates ranging from 175 to 200 per 100,000 population (Fig. 1B, C; counties shaded in red). Of the remaining counties, 6 neighboring counties belonged to cluster **2** (counties shaded in yellow), and the rest of upstate counties were included in the cluster **3** (counties shaded in green) with a death rate < 50 per 100,000 population. Thus, clustering the counties followed by visual inspection revealed that higher COVID-19 infections and deaths were from the counties located in downstate NY (Fig. 1C).

A similar pattern in the distribution of counties in the clusters for COVID-19 infection and death suggests an association between these two variables, which was confirmed from the scatter plot (Fig. 2A) and a strong positive correlation (Pearson's correlation; $r = 0.92$, $P < 0.0001$). The observation suggests that the number of infections in a county is a key determinant for the number of COVID-19 deaths.

Even though we observed a strong correlation between the infection and death rates, this data does not provide information about the disease fatality, that is the proportion of deaths occurring from infections. When the fatality rate (expressed as deaths per 10,000 infections) was calculated for all counties and plotted against the infection rate, a distinct pattern of relationship between these two variables was found (Fig. 2B). We observed that the counties with a high fatality rate had a relatively low infection rate while the counties with high infection rates had a relatively low fatality rate. In accordance, when the counties were divided into three clusters on the basis of infection and fatality rate using a two-dimensional k-means clustering method, we obtained clusters with the following features (Fig. 2B): (1) High fatality and low infection rate (cluster **1**); (2) high infection and low fatality rate (cluster **2**); (3) low infection and low fatality rate (cluster **3**). Interestingly, the locations of the counties included in cluster **1** (Hamilton, Steuben, Tioga, Yates, Orleans, and Warren) were distributed across the NYS (Fig. 2C; counties shaded in red). The counties in cluster **2** (Fig. 2C; counties shaded in yellow) were all in proximity and located near the NYC, although in terms of the fatality rate, they were interspersed with cluster **3** (Fig. 2C; counties shaded in green). Since high fatality from COVID-19 is observed among nursing residents (Rada, 2020), we also checked whether the distribution of nursing homes has a contribution to the variation of fatality observed between NYS counties. Mapping the nursing homes in individual counties, we did not find an apparent relationship between counties with high fatality and increased density of nursing homes (Fig. 2C). These results suggest that various risk factors for COVID-19 have a differential contribution on infection and fatality.

3.2. Impact of demographic factors on COVID-19

Multiple studies have shown the association of demographic variables with COVID-19 infection and outcome (Goldstein and Lee, 2020; Karmakar et al., 2021; Perone, 2021; Sorci et al., 2020). To study how they vary across the clusters of NYS counties that we constructed on the basis of COVID-19 infection, death, and fatality, we selected five well-known demographic risk factors namely, population density, age (percentage of people with age above 55 yr), ethnicity (percentage of African American and Hispanic American population), and poverty (percentage of the population with income below poverty line). Additionally, we considered the distance from the disease epicenter, measured as the distance of a county from Manhattan in NYC. Fig. 3 shows these variables plotted against counties organized in three clusters as described in the previous section. Each variable demonstrated a

Fig. 1. Infection and death from COVID-19 in NYS counties (data till May 16, 2020). (A-B) Infection rates (A) and death rates (B) in individual counties, which are further grouped into three clusters using k-means clustering technique. (Clusters **1, 2,** and **3** represent the counties with high, intermediate, and low infection or death) (C) Maps of NYS showing the locations of counties in each cluster.

characteristic pattern of distribution within the clusters. KW test followed by multiple comparisons was further performed to calculate the statistical difference.

The trends for most demographic variables followed a similar pattern for infection and death clusters except for poverty. For population density and ethnicity (African American or Hispanic American) median values showed a decreasing trend from cluster **1** to cluster **3**, while an opposite trend was observed for age and distance from the epicenter (Fig. 3). Furthermore, the difference between clusters **1** and **2** was not significant for these variables but their difference with cluster **3** was found to be significant (except between clusters **2** and **3** for age). Interestingly, for the percentage of the population below the poverty line, the

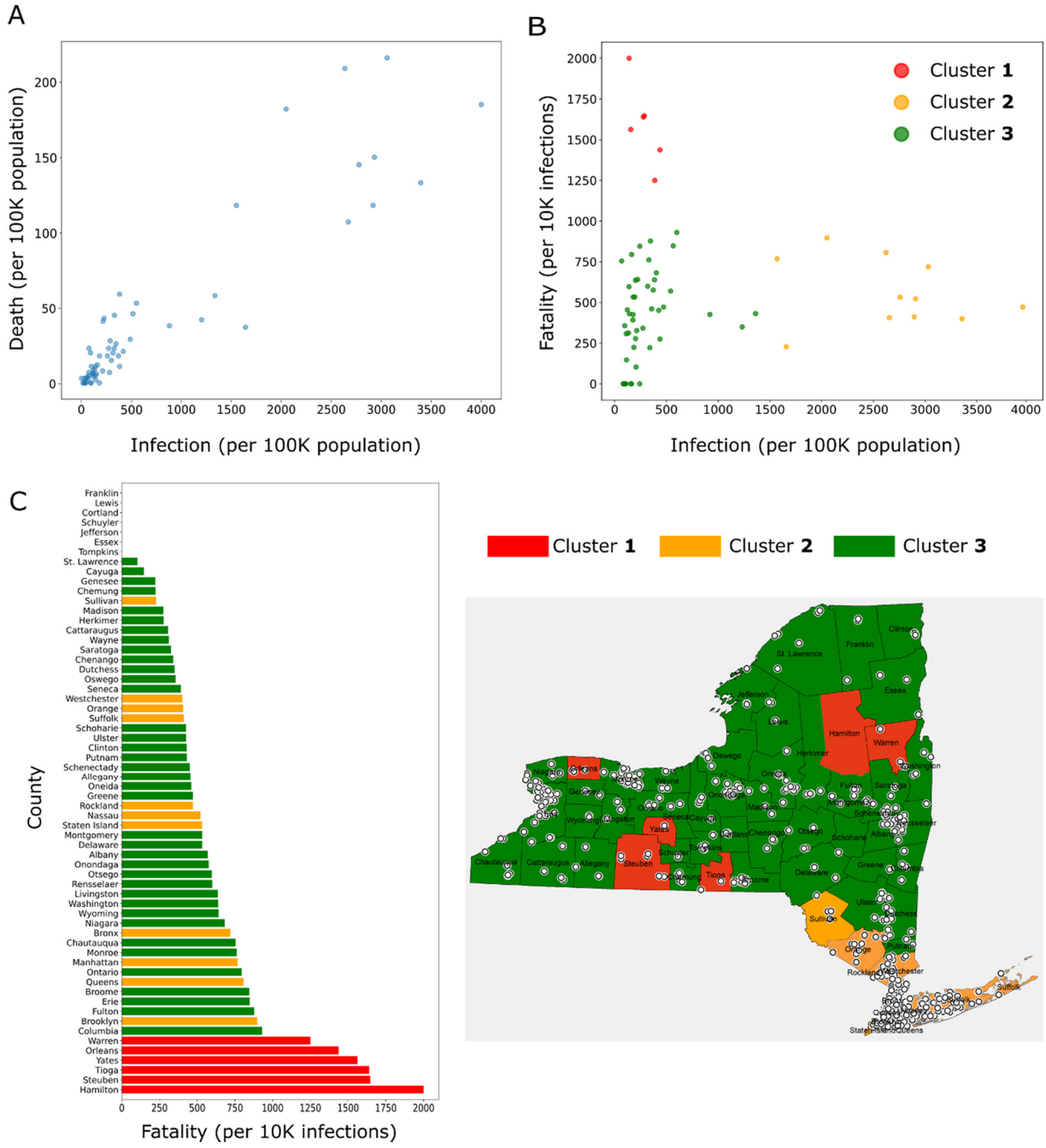

Fig. 2. (A) Scatter plot showing the relationship between COVID-19 infection and death rates in NYS counties. (B) Fatality rate is plotted against infection rate for each county; the counties are further grouped for fatality into 3 clusters using two-dimensional k-means clustering method. Cluster **1** includes counties with high fatality and low infection; cluster **2** includes counties with low fatality and high infection; cluster **3** includes counties with low fatality and low infection. (C) Fatality rates of the counties with the clusters indicated by color *(left);* map of NYS showing the locations of counties belonging to each cluster *(right)*. Locations of nursing homes are also depicted in the map by white circles.

highest median value was observed in cluster **2** for the infection group, and in cluster **1** for the death group; the median values in cluster **3** was intermediate for both infection and death groups, thus, suggesting a role of poverty on COVID-19 infection and death cannot be explained through simple association.

The clusters in the fatality group demonstrated a highly distinct pattern of association with demographic variables (Fig. 3). For all variables except poverty, the median values of cluster **3** (low fatality and low infection) were found to be intermediate between the median values of cluster **1** (high fatality and low infection) and cluster **2** (low fatality and high infection). Specifically, for the percentage of population with age over 55 yr, the highest median value was observed in cluster **1** (36.5%) in comparison to 28.9% and 33.7% observed in cluster **2** and cluster **3**, respectively. For population density and ethnicity, the trend was opposite with cluster **2** and cluster **1** showing the highest and lowest median values among the clusters, respectively (Fig. 3). These findings indicate that high fatality and infections are associated with different sets of demographic risk factors. Overall, the analysis suggests a potential role of demographic structure toward the extent of observed infection, death, and fatality from COVID-19.

3.3. Impact of environmental factors on COVID-19

Since several recent studies have shown an association of environmental factors such as air pollution and temperature on COVID-19 transmission and severity (Li et al., 2020; Wu et al., 2020), we

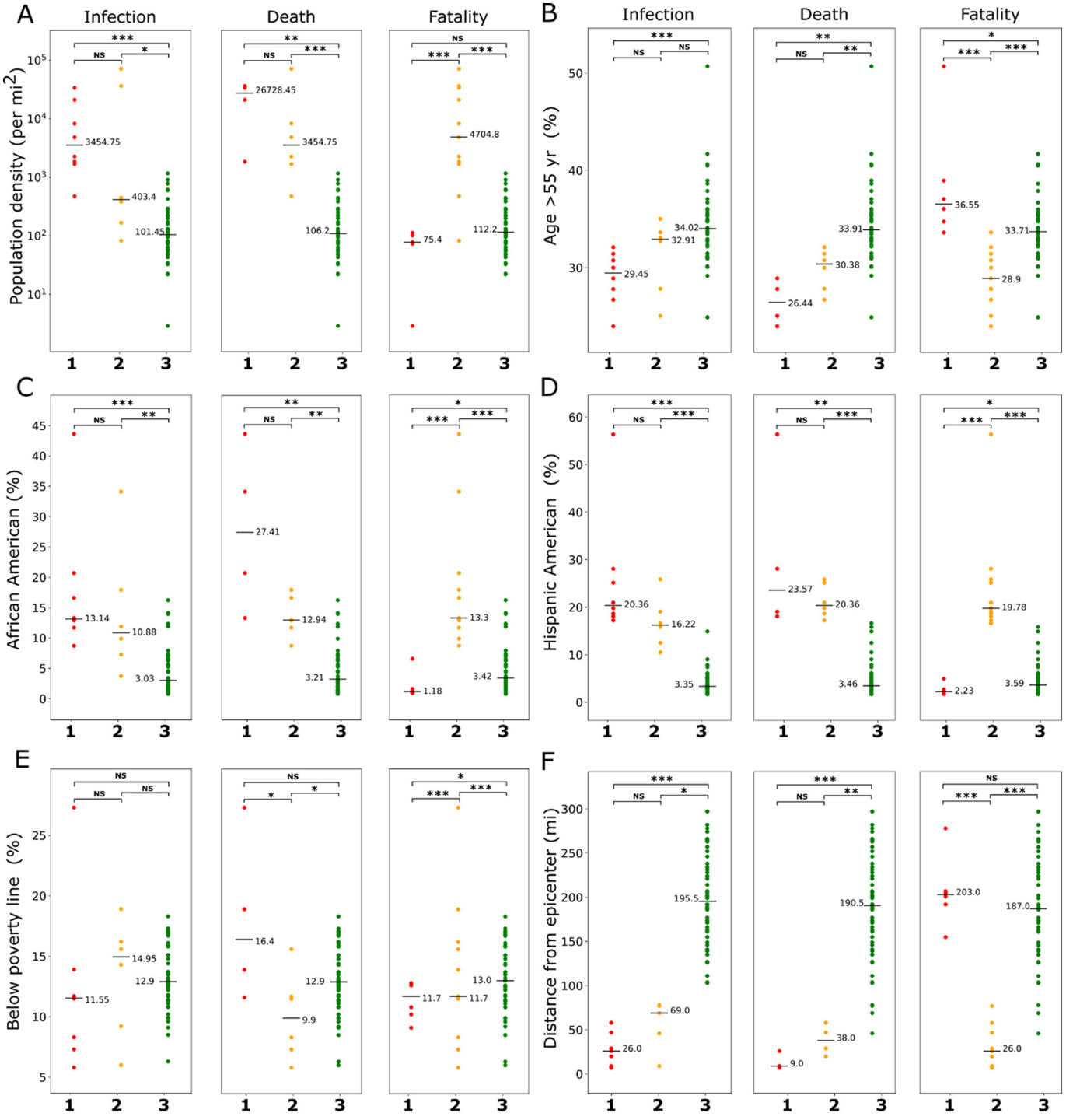

Fig. 3. Association of demographic variables with COVID-19. Counties grouped into clusters by infection, death, or fatality were compared for (A) population density, (B) age (> 55 yr), (C) African American population, (D) Hispanic American population, (E) population below poverty line, and (F) distance from epicenter. Horizontal bars represent medians. $^{***}P < 0.01$, $^{**}P < 0.05$, $^{*}P < 0.10$, NS not significant (Kruskal-Wallis test followed by Mann-Whitney *U* test with Bonferroni corrections). For infection and death category, clusters **1**, **2**, and **3** represent high, intermediate, and low rates of infection or death; for fatality category, cluster **1** indicates high fatality and low infection, cluster **2** indicates low fatality and high infection, and cluster **3** indicates low fatality and low infection.

investigated whether such association could be observed across the clusters of NYS counties. Furthermore, we hypothesized chronic exposure to have a stronger impact than acute exposure. This prompted us to select one EPA site representative for each cluster and collect temperature and AQI data for the years 2015–2019. To compare the variables between the sites and find out any differences throughout the year or any specific period of the year, ARIMA models were constructed from weekly time series data. Fig. 4 shows ARIMA models of predicted values with 95% confidence bands for temperature and AQI. The AIC values of the models for all conditions were low and comparable (range 289.68–303.11), confirming the model robustness. The model predicted temperatures showed a similar pattern for all three clusters in all three categories of infection, death, and fatality with values reaching a peak during the summer months of June–August. Although the predicted temperature for cluster **3** in the infection and the death categories were slightly lower than the other two clusters, there was a

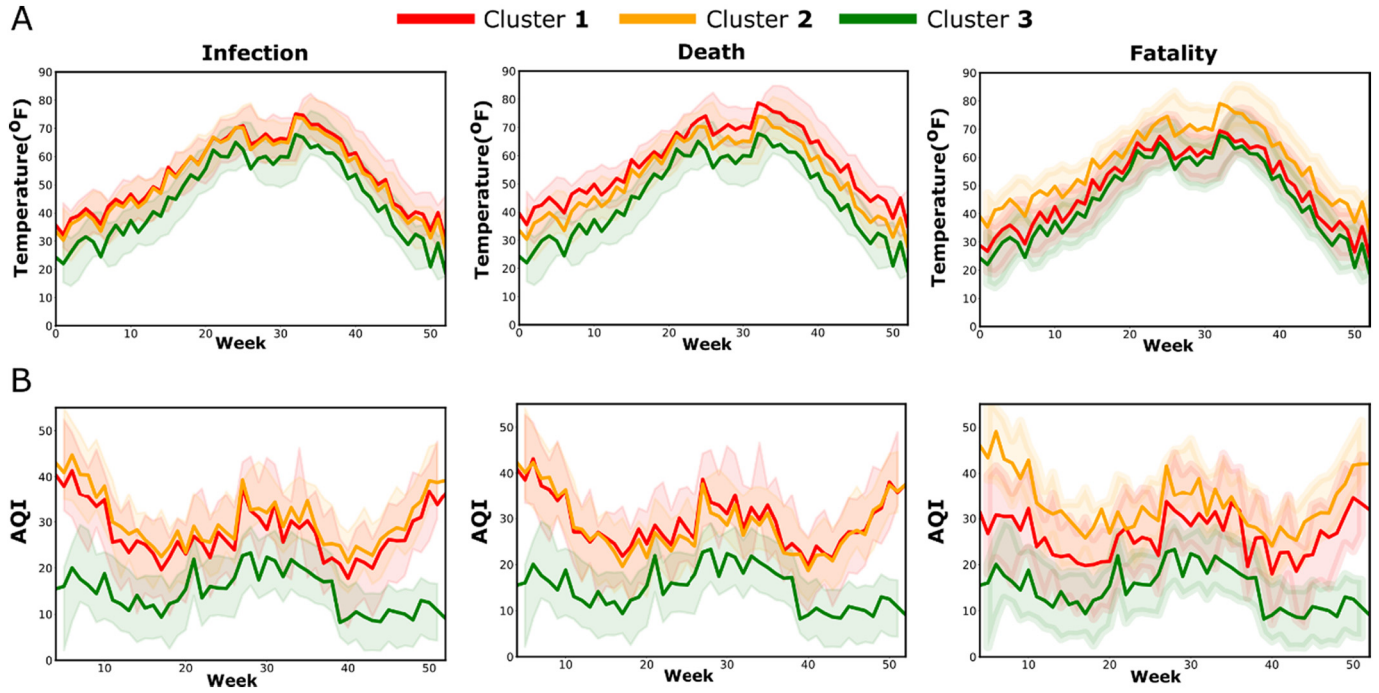

Fig. 4. ARIMA time series analysis of temperature (A) and air AQI (B) from weekly EPA data (2015–2019). Predicted values with 95% confidence band for one year, starting from January are shown in the plots. EPA sites for each cluster were located in a representative county belonging to that cluster. For infection and death categories, clusters **1**, **2**, and **3** represent high, intermediate, and low rates of infection or death; for fatality category, cluster **1** indicates high fatality and low infection, cluster **2** indicates low fatality and high infection, and cluster **3** indicates low fatality and low infection. Abbreviations: ARIMA, autoregressive integrated moving average; AQI, air quality index.

considerable overlap of the confidence bands, thus an association the clusters with temperature could not be inferred (Fig. 4A). Similarly, the confidence bands of the models for temperature in the fatality clusters also demonstrated a substantial overlap. In contrast to temperature, the model predicted AQI values demonstrated a larger separation between the clusters (Fig. 4B). In the infection and death groups, AQI values for cluster **3** were substantially lower than the values for clusters **1** and **2**, and the differences were more prominent during the winter months with separation of the confidence bands. In the fatality group, the highest AQI values were observed in the cluster **2**, which corresponds to high infection but low fatality, and the lowest AQI values were observed in the cluster **3**, corresponding to low infection and low fatality. Thus, the analysis of EPA data suggests COVID-19 in NYS is linked to poor air quality but not with outdoor temperature.

Although EPA measurements provide an accurate estimate of the air quality, data at the resolution of individual counties are not available due to the relatively few EPA sampling sites across the NYS. Therefore, to capture the variation of air quality across the counties, we used temporally averaged $PM_{2.5}$ estimates from satellite data and ground-based measurements over a time period of 2000–2016 (Wu et al., 2020). When the $PM_{2.5}$ values from the counties were compared between the COVID-19 clusters for infection, death, and fatality, the pattern corroborated well with the observations from EPA data (Fig. 5). For COVID-19 infection and death, $PM_{2.5}$ values of counties in cluster **3** were significantly lower than the counties in clusters **1** and **2**, with no significant difference observed between the latter two. Similar to the findings with EPA data, in the fatality group, the $PM_{2.5}$ of counties in cluster **2** was significantly higher than in cluster **1** and **3**. These findings demonstrate the association of $PM_{2.5}$ with COVID-19 infection and death in the NYS.

3.4. Contributions of risk factors on COVID-19 infection, death, and fatality

Since clustering of counties based on COVID-19 infection, death, or fatality demonstrated a distinct pattern of association with demographic or environmental risk factors, we wanted to further elucidate the contribution of these variables on the specific aspects of COVID-19 burden. Six risk factors namely, age above 55 yr, ethnicity (African American and Hispanic American population), poverty, population density, distance from the epicenter, and $PM_{2.5}$ were considered as predictor variables, and multivariate regression model with forward "stepwise" selection was used for analysis. Three separate models were constructed using infection, death, and fatality rate as dependent variables to understand the relative contribution of the risk factors for each of these outcomes. Rockland county was excluded from the models as it was identified as an outlier while performing residual analyses of the regression output.

Multicollinearity among the predictor variables can lead to unstable and unreliable estimates of regression coefficients, reducing the power of the regression model. Therefore, before their incorporation in the regression models, we checked for multicollinearity. The correlation matrices in Fig. 6A show the Pearson's correlations coefficients among variable pairs. A strong positive correlation was found between ethnicity and $PM_{2.5}$ ($r = 0.81, P < 0.001$), while moderate positive correlations were observed between population density and $PM_{2.5}$, ($r = 0.69$, $P < 0.001$) or ethnicity ($r = 0.67, P < 0.001$). Additionally, ethnicity and $PM_{2.5}$ demonstrated a strong positive correlation with infection and death, while the distance from the epicenter held a strong negative correlation with these dependent variables. Interestingly, such strong correlations were not observed for fatality, the third dependent variable.

The existence of multicollinearity among predictor variables prompted us to calculate the VIF for each variable to assess their suitability for inclusion in the regression model. We found that VIFs of all variables were lower than the acceptable cut-off value of 5, except for ethnicity when infection or death was used as dependent variables. This implies that ethnicity is not an independent predictor for infection and death, and therefore, was excluded in the regression models for these two variables. The models revealed distinct contributions of the predictor variables to infection, death, and fatality rates (Fig. 6B). $PM_{2.5}$ and distance from the epicenter were found to be the two most important predictors for infection and death. For infection rate,

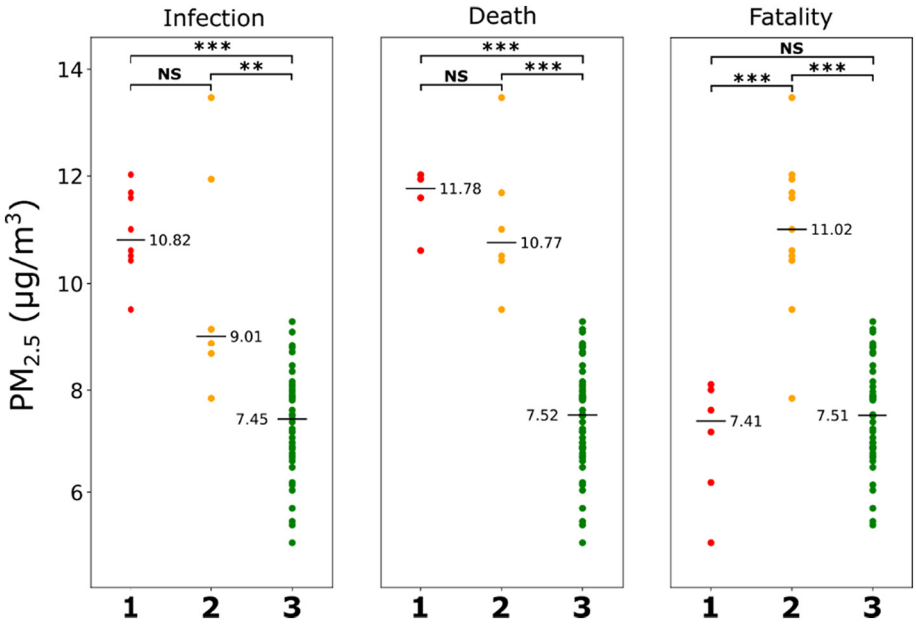

Fig. 5. Temporally averaged $PM_{2.5}$ estimates from NYS counties for the years 2000–2016 are compared between clusters based on COVID-19 infection, death, and fatality. Horizontal lines represent median values. $^{***}P < 0.01$, $^{**}P < 0.05$, $^{*}P < 0.10$, NS not significant (Mann-Whitney *U* test with Bonferroni corrections). For infection and death categories, clusters **1**, **2**, and **3** represent high, intermediate, and low rates of infection or death; for fatality category, cluster **1** indicates high fatality and low infection, cluster **2** indicates low fatality and high infection, and cluster **3** indicates low fatality and low infection.

distance from the epicenter was the strongest predictor with a highly significant regression coefficient ($P < 0.001$, Fig. 6C) and generated an adjusted R^2 value of 0.60 when considered as a sole contributor of the model (Fig. 6B); the adjusted R^2 value increased to 0.71 following the inclusion of $PM_{2.5}$ in the model, which also had a significant regression coefficient ($P < 0.001$; Fig. 6B, C). Regression coefficients of population density, age, and poverty emerged as not significant ($P > 0.05$) and their addition to the regression model only marginally increased the adjusted R^2 value 0.74. Similar to infection, distance from the epicenter and $PM_{2.5}$ were two major predictors for the death rate, however, $PM_{2.5}$ was the strongest among them contributing to an adjusted R^2 value of 0.69. The value increased to 0.73 following the inclusion of distance from the epicenter in the model but did not change further upon the addition of other variables.

Unlike the models for infection and death rates, age over 55 yr was found to be the strongest predictor in the model for fatality rate, (Fig. 6B, C). $PM_{2.5}$ was the second major predictor in the model, although the relatively high *P*-value (0.074) of the regression coefficient suggests a weaker link with fatality. It should also be noted that the adjusted R^2 value of the final model for fatality was 0.26, indicating that the goodness of model fit is much lower than the other two models for infection and death. Together, the regression analysis helped to delineate the risk factors with major contributions on specific aspects of the COVID-19 burden.

4. Discussion

Our analysis has shown a wide heterogeneity in the infection, death, and fatality rates from COVID-19 among the counties in the NYS during the first pandemic wave. Infection was found to be strongly correlated with death but not with fatality. By grouping the counties into clusters, we show the association of multiple demographic factors and air quality with infection, death, and fatality from COVID-19. Specifically, $PM_{2.5}$, population density, and proportion of African American or Hispanic American population demonstrated a positive association with infection and death, while the distance from the disease epicenter showed a negative association. In contrast, higher fatality from the disease was primarily associated with a higher proportion of the population aged above 55 yr. Furthermore, regression analysis has identified the major contributors among these risk factors for infection, death, and fatality. These results could help to better understand the impact of environmental and demographic factors on COVID-19 in NYS.

Our analysis shows an association of $PM_{2.5}$ with infection and death, a potential but weaker link to fatality. This finding is in agreement with studies focused on the role of outdoor air pollution on COVID-19 transmission and health outcomes (Benmarhnia, 2020; Gupta et al., 2020; Lolli et al., 2020; Pozzer et al., 2020; Wu et al., 2020). $PM_{2.5}$ has been reported to be positively correlated with both increased COVID-19 transmission and fatality. Comorbid conditions such as respiratory and cardiovascular illnesses that are associated with chronic exposure to higher $PM_{2.5}$ are thought to aggravate the illness from virus infection, posing a higher risk of death (Benmarhnia, 2020; Pozzer et al., 2020; Wu et al., 2020). Additional mechanisms proposed for increased SARS-CoV-2 transmission by $PM_{2.5}$ include the particulate matters serving as a transport vector and their ability to increase the susceptibility to infection by inducing lung inflammation (Maleki et al., 2021). It is to be noted that although the average $PM_{2.5}$ values in the NYS meet the safe limit ($< 12\ \mu g/m^3$) set by EPA (Jin et al., 2019), an association of $PM_{2.5}$ level with adverse COVID-19 outcome can be clearly discerned. We attribute this apparent discrepancy to the existence of potential hot spots where the exposure $PM_{2.5}$ could be much higher than the average. Although our analysis considers chronic exposure to $PM_{2.5}$ (average values from 2000 to 2016) to better capture the long-term health effects(Wu et al., 2020), a recent study showed no significant difference in air quality in the NYC area after lockdown (Zangari et al., 2020), and thus would also reasonably reflect the exposure to $PM_{2.5}$ during the period of investigation. Also, our work focuses on $PM_{2.5}$ alone, however, other air pollutants, especially NO_2 and O_3 are reported to be associated with higher COVID-19 spread and fatality (Adhikari and Yin, 2020; Copat et al., 2020; Liang et al., 2020). Commonly generated by anthropogenic activities such as traffic, NO_2 is a well-known inducer of lung inflammation and can synergistically act with $PM_{2.5}$ to increase the adverse impact of COVID-19 (Hesterberg et al., 2009; Huang et al., 2012). NO_2 is also a source for O_3 formation,

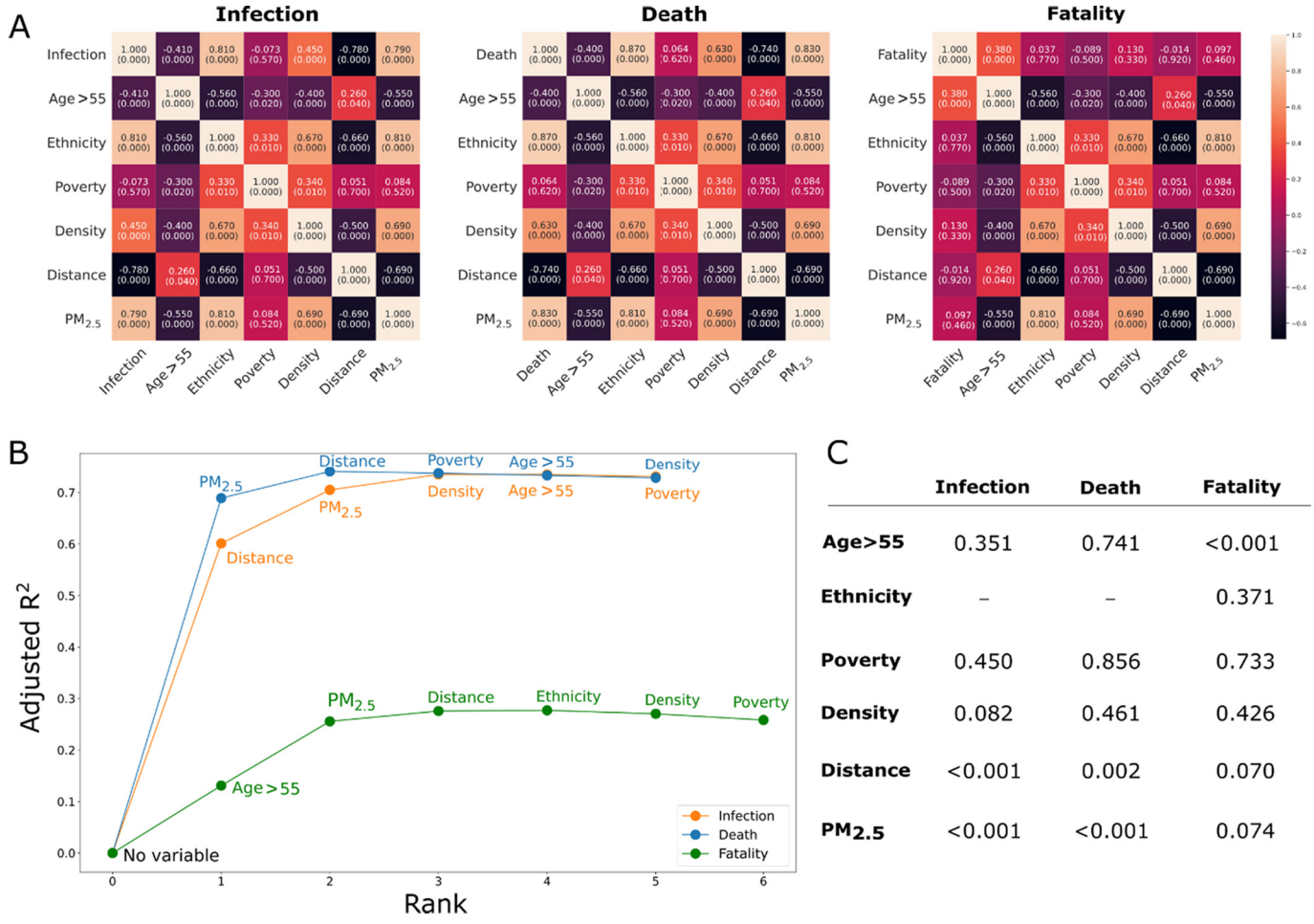

C

	Infection	Death	Fatality
Age>55	0.351	0.741	<0.001
Ethnicity	–	–	0.371
Poverty	0.450	0.856	0.733
Density	0.082	0.461	0.426
Distance	<0.001	0.002	0.070
$PM_{2.5}$	<0.001	<0.001	0.074

Fig. 6. Regression analysis to assess relative contribution of risk factors on COVID-19 infection, death, and fatality. (A) Correlation matrices between demographic risk variables and $PM_{2.5}$ for infection, death, and fatality. Pearson's correlations coefficients between the variables are shown with corresponding *P* values are mentioned in the parentheses. (B) Stepwise regression model with forward selection for infection, death, and fatality. (Note that ethnicity is excluded from the models for infection and death due to the existence of strong multicollinearity). (C) Table showing the P values of the regression coefficients from the analysis. Abbreviations used: Density, population density (per mi^2); Ethnicity, African American and Hispanic American (%); Poverty, population below poverty line (%); Distance, distance from the epicenter (mi).

which is further facilitated by higher temperature and $PM_{2.5}$ (Zhang et al., 2019). O_3 is a strong oxidant and exposure to O_3 is known to cause or aggravate respiratory and cardiovascular diseases, and older adults are shown to be more vulnerable to the adverse effects (Day et al., 2018; Zhang et al., 2019). Thus, apart from independent effects, the interactions of NO_2 and O_3 with $PM_{2.5}$ could be important in the context of COVID-19 and needs to be investigated in the future study. Outdoor air temperature, the other environmental parameter we examined in this study, did not show any association with COVID-19 cases; both positive and negative association of temperature with COVID-19 infection have been reported in the literature, and a recent systematic review concluded data-related and methodological issues including inherent uncertainties of the data, inappropriate controlling for confounding parameters, and short periods of investigation underlie such conflicting results (Dong et al., 2021; Lolli et al., 2020). Thus, to better understand the influence of temperature on COVID-19, future studies should be conducted with time-resolved data for a longer period and taking appropriate measures for confounding variables.

We observed a strong correlation between $PM_{2.5}$ and the percentage of the population belonging to African American or Hispanic American ethnicity ($r = 0.81$, $P < 0.001$), suggesting that people from these ethnicities are exposed to a higher level of $PM_{2.5}$ than the average population. Multiple studies have concluded that these two ethnicities in the US are at disproportionately higher risk of COVID-19 (Cordes and Castro, 2020; Li et al., 2020; Martinez et al., 2020; Yancy, 2020). Factors related to socioeconomic inequities such as the greater risk of virus exposure from professional demand or living in crowded accommodation, higher prevalence of chronic comorbidity, and restricted access to healthcare are thought to underlie such differences (Patel et al., 2020). Our results suggest that exposure to air pollution could be a contributor to further increase this disparity. Low socioeconomic status is thought to pose a greater risk for COVID-19 exposure (Yancy, 2020); however, for NYS, we observed counties in cluster **3** for infection and death rates to have a higher proportion of people living below the poverty line than the counties from other two clusters. That cluster **3** counties have a relatively lower risk from other demographic and environmental variables could explain this apparent discrepancy. Indeed, when considering the population of NYC alone, poverty and COVID-19 are found to be positively correlated (Cordes and Castro, 2020).

Two demographic variables, distance from the epicenter and age above 55 years, came out as major contributors in our regression models. However, their influences on COVID-19 were distinct. The distance of counties from the disease epicenter was inversely related to infection and death, alone accounting for 60% of variation in the regression model of infection. This finding is not unusual as the disease spread would be facilitated by the population mobility with the highest effect on the neighboring regions. We also observed a strong correlation between infection and death rates ($r = 0.92$, $P < 0.0001$), corroborating their association with a similar set of risk factors. In contrast, a poor

correlation was observed between infection and fatality, and the regression model for fatality revealed age over 55 years to be the most significant independent variable. Fatality from COVID-19 depends on the health of patients where age plays a crucial role (Mesas et al., 2020; Richardson et al., 2020). Increased risk of the aged population to complications and death from COVID-19 is observed across the world, and multiple factors including the existence of chronic comorbid conditions and a weaker immune system are thought to underlie such vulnerability (Mesas et al., 2020). The association of distinct sets of risk factors for death and fatality suggests that they should be considered as separate metrics for the COVID-19 burden for the development of preventive or mitigative strategies.

Grouping the counties into clusters not only helped to visualize how NYS counties are impacted by specific COVID-19 adversities but also allowed easier comparison of their association with various demographic and environmental risk variables. While the regression models have further helped to identify the risk variables that have major contributions to specific aspects of disease impact, it should also be noted that the adjusted R^2 value of the regression model for fatality is substantially lower than the models for infection and death (0.26 vs. 0.74 and 0.73). This difference suggests the possibility of missing key variables in the model for COVID-19 fatality that needs to be identified and incorporated in the future model. Such variables could potentially be the measures pertaining to the outcome of an infected individual, including the availability and access to healthcare resources, vaccination, and awareness for early diagnosis and treatment.

5. Conclusions

In this work, we analyzed the association of multiple demographic and environmental factors with the COVID-19 burden in NYS during the first pandemic wave. Clustering the counties based on COVID-19 infection or death revealed their segregation by geographical location with clusters located farther away from NYC showing lower infection or death. In contrast, counties grouped in the cluster for high disease fatality were distributed across the NYS and were different from those having high infection and death rates. The clustered counties showed a prominent association with demographic variables and $PM_{2.5}$ but the patterns of association for infection and death were distinct compared to fatality. Clusters with high infection and death were found to have higher $PM_{2.5}$, higher population density, a higher proportion of African Americans and Hispanic Americans, and were closer to the disease epicenter, while the cluster with higher fatality had a higher proportion of population aged above 55 yr. Stepwise regression models built on county data further showed that $PM_{2.5}$ and the distance from the epicenter are two major contributors for infection and death, while advanced age makes the strongest contribution to fatality. Although our study is confined to counties within the NYS, we observed prominent differences in the distribution of infection and fatality along with an association with distinct sets of demographic and environmental risk variables. The US being a country with a vast size, consisting of considerable heterogeneity between states in terms of social and cultural practices, public health policies, access to healthcare, and general awareness of COVID-19, all of which could have a significant impact on the absolute magnitude of COVID-19 burden; however, we expect that the variables considered in this work would still have similar effects as observed for the NYS, and thus, our results can provide key insight on the contribution of demographic and environmental factors on the disease landscape in these states. Additionally, a similar modeling approach could be utilized in future studies to include additional relevant variables in the analysis to understand their contribution to the disease. With strong anthropogenic contributions to the environment in modern societies, our findings suggest the need for critical consideration of both demographic and environmental variables when predicting the impact of COVID-19 or developing preventive or mitigative strategies to control the disease.

Funding information

Not applicable.

CRediT authorship contribution statement

Sumona Mondal: Writing – original draft, Supervision, Methodology, Formal analysis, Project administration. **Chaya Chaipitakporn:** Formal analysis, Visualization, Data Curation. **Bridget Wangler**: Visualization. **Vijay Kumar**: Data curation. **Supraja Gurajala**: Review and editing. **Suresh Dhaniyala**: Validation, Review and editing. **Shantanu Sur**: Conceptualization, Investigation, Supervision, Writing - review and editing.

Declaration of competing interest

The authors declare that they have no known competing financial interests or personal relationships that could have appeared to influence the work reported in this paper.

Acknowledgments

Vijay Kumar acknowledges the support from US-Pakistan Knowledge Corridor PhD Scholarship Program under Higher Education Commission, Pakistan. Bridget Wangler thanks the Clarkson University Honors Program for their support.

References

Adhikari, A., Yin, J., 2020. Short-term effects of ambient ozone, PM2.5, and meteorological factors on COVID-19 confirmed cases and deaths in Queens, New York. Int. J. Environ. Res. Public Health 17, 4047.

Arif, M., Sengupta, S., 2020. Nexus between population density and novel coronavirus (COVID-19) pandemic in the south indian states: a geo-statistical approach. Environ. Dev. Sustain. 1–29.

Auger, K.A., Shah, S.S., Richardson, T., Hartley, D., Hall, M., Warniment, A., et al., 2020. Association between statewide school closure and COVID-19 incidence and mortality in the US. JAMA 324, 859–870.

Baldwin, R., Di Mauro, B.W., 2020. Economics in the Time of COVID-19: A New eBook. CEPR Press.

Bashir, M.F., Ma, B.J., Bilal, Komal B., Bashir, M.A., Tan, D.J., et al., 2020. Correlation between climate indicators and COVID-19 pandemic in New York, USA. Sci. Total Environ. 728, 138835.

Benmarhnia, T., 2020. Linkages between air pollution and the health burden from COVID-19: methodological challenges and opportunities. Am. J. Epidemiol. 189, kwaa148.

Brook, R.D., Rajagopalan, S., Pope, C.A., Brook, J.R., Bhatnagar, A., Diez-Roux, A.V., et al., 2010. Particulate matter air pollution and cardiovascular disease. Circulation 121, 2331–2378.

Chatterjee, S., Simonoff, J.S., 2013. Handbook of Regression Analysis. vol. 5. John Wiley & Sons.

Chauhan, A.J., Johnston, S.L., 2003. Air pollution and infection in respiratory illness. Br. Med. Bull. 68, 95–112.

Chen, J.T., Krieger, N., 2021. Revealing the unequal burden of COVID-19 by income, race/ethnicity, and household crowding: US County versus zip code analyses. J. Public Health Manag. Pract. 27 (Suppl. 1), S43–S56.

Copat, C., Cristaldi, A., Fiore, M., Grasso, A., Zuccarello, P., Signorelli, S.S., et al., 2020. The role of air pollution (PM and NO2) in COVID-19 spread and lethality: a systematic review. Environ. Res. 191, 110129.

Copiello, S., Grillenzoni, C., 2020. The spread of 2019-nCoV in China was primarily driven by population density. Comment on "Association between short-term exposure to air pollution and COVID-19 infection: evidence from China" by Zhu et al. Sci. Total Environ. 744, 141028.

Cordes, J., Castro, M.C., 2020. Spatial analysis of COVID-19 clusters and contextual factors in New York City. Spat. Spatio-temporal Epidemiol. 34, 100355.

Day, D.B., Clyde, M.A., Xiang, J., Li, F., Cui, X., Mo, J., et al., 2018. Age modification of ozone associations with cardiovascular disease risk in adults: a potential role for soluble P-selectin and blood pressure. J. Thorac. Dis. 10, 4643–4652.

Dong, Z.M., Fan, X.R., Wang, J., Mao, Y.X., Luo, Y.Y., Tang, S., 2021. Data-related and methodological obstacles to determining associations between temperature and COVID-19 transmission. Environ. Res. Lett. 16, 034016.

Donkelaar, A.V., Martin, R.V., Li, C., Burnett, R.T., 2019. Regional estimates of chemical composition of fine particulate matter using a combined geoscience-statistical method with information from satellites, models, and monitors. Environ. Sci. Technol. 53, 2595–2611.

Fahim, A.M., Salem, A.M., Torkey, F.A., Ramadan, M.A., 2006. An efficient enhanced k-means clustering algorithm. J. Zhejiang Univ. Sci. A 7, 1626–1633.

Feng, C., Li, J., Sun, W., Zhang, Y., Wang, Q., 2016a. Impact of ambient fine particulate matter (PM2.5) exposure on the risk of influenza-like-illness: a time-series analysis in Beijing, China. Environ. Health 15, 17.
Feng, S., Gao, D., Liao, F., Zhou, F., Wang, X., 2016b. The health effects of ambient PM2.5 and potential mechanisms. Ecotoxicol. Environ. Saf. 128, 67–74.
Goldstein, J.R., Lee, R.D., 2020. Demographic perspectives on the mortality of COVID-19 and other epidemics. Proc. Natl. Acad. Sci. U. S. A. 117, 22035–22041.
Guan, W.J., Zheng, X.Y., Chung, K.F., Zhong, N.S., 2016. Impact of air pollution on the burden of chronic respiratory diseases in China: time for urgent action. Lancet 388, 1939–1951.
Gupta, A., Bherwani, H., Gautam, S., Anjum, S., Musugu, K., Kumar, N., et al., 2020. Air pollution aggravating COVID-19 lethality? Exploration in Asian cities using statistical models. Environ. Dev. Sustain. 1–10.
Hesterberg, T.W., Bunn, W.B., McClellan, R.O., Hamade, A.K., Long, C.M., Valberg, P.A., 2009. Critical review of the human data on short-term nitrogen dioxide (NO2) exposures: evidence for NO2 no-effect levels. Crit. Rev. Toxicol. 39, 743–781.
Hopke, P.K., Croft, D., Zhang, W., Lin, S., Masiol, M., Squizzato, S., et al., 2019. Changes in the acute response of respiratory diseases to PM2.5 in New York State from 2005 to 2016. Sci. Total Environ. 677, 328–339.
Huang, Y.C., Rappold, A.G., Graff, D.W., Ghio, A.J., Devlin, R.B., 2012. Synergistic effects of exposure to concentrated ambient fine pollution particles and nitrogen dioxide in humans. Inhal. Toxicol. 24, 790–797.
Hyndman, R.J., Athanasopoulos, G., 2018. Forecasting: Principles and Practice: OTexts.
Jin, X.M., Fiore, A.M., Civerolo, K., Bi, J.Z., Liu, Y., van Donkelaar, A., et al., 2019. Comparison of multiple PM2.5 exposure products for estimating health benefits of emission controls over New York State, USA. Environ. Res. Lett. 14, 084023.
Karmakar, M., Lantz, P.M., Tipirneni, R., 2021. Association of social and demographic factors with COVID-19 incidence and death rates in the US. JAMA Netw. Open 4, e2036462.
Lee, V.J., Chiew, C.J., Khong, W.X., 2020. Interrupting transmission of COVID-19: lessons from containment efforts in Singapore. J Travel Med 27.
Li, A.Y., Hannah, T.C., Durbin, J.R., Dreher, N., McAuley, F.M., Marayati, N.F., et al., 2020. Multivariate analysis of black race and environmental temperature on COVID-19 in the US. Am J Med Sci 360, 348–356.
Liang, D., Shi, L., Zhao, J., Liu, P., Sarnat, J.A., Gao, S., et al., 2020. Urban air pollution may enhance COVID-19 case-fatality and mortality rates in the United States. Innovation 1, 100047.
Liu, J., Zhou, J., Yao, J., Zhang, X., Li, L., Xu, X., et al., 2020. Impact of meteorological factors on the COVID-19 transmission: a multi-city study in China. Sci. Total Environ. 726, 138513.
Lolli, S., Chen, Y.C., Wang, S.H., Vivone, G., 2020. Impact of meteorological conditions and air pollution on COVID-19 pandemic transmission in Italy. Sci. Rep. 10, 16213.
Lusignan, Sd., Dorward, J., Correa, A., Jones, N., Akinyemi, O., Amirthalingam, G., et al., 2020. Risk factors for SARS-CoV-2 among patients in the Oxford Royal College of General Practitioners Research and Surveillance Centre primary care network: a cross-sectional study. Lancet Infect. Dis. 20, 1034–1042.
Maleki, M., Anvari, E., Hopke, P.K., Noorimotlagh, Z., Mirzaee, S.A., 2021. An updated systematic review on the association between atmospheric particulate matter pollution and prevalence of SARS-CoV-2. Environ. Res. 195, 110898.
Martinez, D.A., Hinson, J.S., Klein, E.Y., Irvin, N.A., Saheed, M., Page, K.R., et al., 2020. SARS-CoV-2 positivity rate for Latinos in the Baltimore-Washington, DC Region. JAMA 324, 392–395.
Mesas, A.E., Cavero-Redondo, I., Alvarez-Bueno, C., Sarria Cabrera, M.A., Maffei de Andrade, S., Sequi-Dominguez, I., et al., 2020. Predictors of in-hospital COVID-19 mortality: a comprehensive systematic review and meta-analysis exploring differences by age, sex and health conditions. PLoS One 15, e0241742.
Miller, L.E., Bhattacharyya, R., Miller, A.L., 2020. Data regarding country-specific variability in Covid-19 prevalence, incidence, and case fatality rate. Data Brief 32, 106276.
Monmonier, M., Giordano, A., 1998. GIS in New York state county emergency management offices: user assessment. Appl. Geogr. Stud. 2, 95–109.
Patel, J.A., Nielsen, F.B.H., Badiani, A.A., Assi, S., Unadkat, V.A., Patel, B., et al., 2020. Poverty, inequality and COVID-19: the forgotten vulnerable. Public Health 183, 110–111.
Perone, G., 2021. The determinants of COVID-19 case fatality rate (CFR) in the italian regions and provinces: an analysis of environmental, demographic, and healthcare factors. Sci. Total Environ. 755, 142523.
Pozzer, A., Dominici, F., Haines, A., Witt, C., Munzel, T., Lelieveld, J., 2020. Regional and global contributions of air pollution to risk of death from COVID-19. Cardiovasc. Res. 116, 2247–2253.
Pradhan, A., Olsson, P.E., 2020. Sex differences in severity and mortality from COVID-19: are males more vulnerable? Biol. Sex Differ. 11, 53.
Rada, A.G., 2020. Covid-19: the precarious position of Spain's nursing homes. BMJ 369, m1554.
Reichberg, S.B., Mitra, P.P., Haghamad, A., Ramrattan, G., Crawford, J.M., Northwell, C.-R.C., et al., 2020. Rapid emergence of SARS-CoV-2 in the greater New York metropolitan area: geolocation, demographics, positivity rates, and hospitalization for 46 793 persons tested by Northwell Health. Clin. Infect. Dis. 71, 3204–3213.
Richardson, S., Hirsch, J.S., Narasimhan, M., Crawford, J.M., McGinn, T., Davidson, K.W., et al., 2020. Presenting characteristics, comorbidities, and outcomes among 5700 patients hospitalized with COVID-19 in the New York City area. JAMA 323, 2052–2059.
Rocklöv, J., Sjödin, H., 2020. High population densities catalyze the spread of COVID-19. J. Travel Med. 27.
Sarkodie, S.A., Owusu, P.A., 2020a. Global assessment of environment, health and economic impact of the novel coronavirus (COVID-19). Environ. Dev. Sustain. 1–11.
Sarkodie, S.A., Owusu, P.A., 2020b. Impact of meteorological factors on COVID-19 pandemic: evidence from top 20 countries with confirmed cases. Environ. Res. 191, 110101.
Sorci, G., Faivre, B., Morand, S., 2020. Explaining among-country variation in COVID-19 case fatality rate. Sci. Rep. 10, 18909.
U.S. Census Bureau ACS, 2018. American Community Survey 1-Year Estimates, Table DP05. . https://data.census.gov/cedsci/table?q=dp05&tid=ACSDP1Y2018.DP05.
Wadhera, R.K., Wadhera, P., Gaba, P., Figueroa, J.F., Joynt Maddox, K.E., Yeh, R.W., et al., 2020. Variation in COVID-19 hospitalizations and deaths across New York City boroughs. JAMA 323, 2192–2195.
Wellenius, G.A., Burger, M.R., Coull, B.A., Schwartz, J., Suh, H.H., Koutrakis, P., et al., 2012. Ambient air pollution and the risk of acute ischemic stroke. Arch. Intern. Med. 172, 229–234.
Wu, X., Nethery, R.C., Sabath, M.B., Braun, D., Dominici, F., 2020. Air pollution and COVID-19 mortality in the United States: strengths and limitations of an ecological regression analysis. Sci. Adv. 6, eabd4049.
Xing, Y.F., Xu, Y.H., Shi, M.H., Lian, Y.X., 2016. The impact of PM2.5 on the human respiratory system. J. Thorac. Dis. 8, E69–E74.
Yancy, C.W., 2020. COVID-19 and African Americans. JAMA 323, 1891–1892.
Zangari, S., Hill, D.T., Charette, A.T., Mirowsky, J.E., 2020. Air quality changes in New York City during the COVID-19 pandemic. Sci. Total Environ. 742, 140496.
Zhang, J.J., Wei, Y., Fang, Z., 2019. Ozone pollution: a major health hazard worldwide. Front. Immunol. 10, 2518.